

Investigating Shock Wave—Boundary Layer Interaction Caused By Reflecting Detonations

J. Damazo^{1*}, J. Ziegler¹, J. Karnesky², and J. E. Shepherd¹

¹ Graduate Aerospace Laboratories, California Institute of Technology

² Propulsion Directorate, Air Force Research Laboratory

*Corresponding author: damazo@caltech.edu

We consider a pipe or tube containing a flammable gaseous mixture and subjected to an internal detonation. When the detonation impacts the closed end of the tube, a reflected shock wave is created to bring the flow back to rest. This shock propagates into the unsteady flow field behind the detonation. In shock tube experiments, it has been observed (e.g., Mark, 1958; Petersen and Hanson, 2006) that a reflecting shock wave may bifurcate (split into an oblique and normal wave) near the wall when it interacts with the boundary layer created by the incident shock. We suspect an analogous event is occurring in detonation reflection. Pressure records from detonations in stoichiometric ethylene-oxygen at initial pressure 0.5 bar show measured shock speeds that are inconsistent with the measured pressure jump across the reflected shock wave. Highly resolved, two-dimensional numerical simulations of compressible viscous flow demonstrate the bifurcation of the reflecting shock wave from the reflection of an ideal detonation.

Keywords: gaseous detonation, shock reflection, shock wave-boundary layer interaction, computational fluid dynamics, AMROC

1. Introduction

Detonation reflection from the closed end of a pipe or tube will produce a reflected shock wave with a peak pressure about 2.4 times the Chapman-Jouget value (Shepherd et al., 1991). For sufficiently high peak pressures and thin-walled pipes or tubes, plastic deformation (Karnesky, 2010) may result. In extreme cases or if there are flaws in the piping, propagating cracks and tube rupture may result (Chao and Shepherd, 2004).

In our recent studies of structural response to detonation, we observed that the measured peak pressures at the wall were below those consistent with the measured shock wave speeds (Karnesky et al., 2010). This suggests that the reflected shock wave is not planar and a portion of the front is oblique to the tube wall. One way in which this can occur is due to the interaction of the reflected shock wave with the boundary layer created on the wall by the incident detonation.

Previous researchers have investigated the interaction of reflected shock waves with boundary layers in the context of shock tube performance and it has been observed (Mark, 1958; Petersen

and Hanson, 2006) that interaction with the boundary layer may cause the reflecting shock wave to bifurcate into an unaffected normal shock wave and a leading shock wave or “foot” that travels along the tube wall. Mark developed a simple model for predicting conditions under which bifurcation will occur. However, no analogous theory has been developed for detonations and the possible role of the boundary layer in detonation reflection has received relatively little attention in past research (Shepherd et al., 1991). The goal of the present study is to obtain some insights into the effects of shock wave boundary layer interaction on detonation reflection in order to make more realistic models of pressure loads for structural response in finite-element simulations as well as single degree of freedom models such as used by Karnesky et al. (2010).

2. Ideal Detonation Reflection Model

The generation of a reflected shock wave by an ideal detonation wave is shown in Figure 1. The detonation travels from the point of ignition to the tube end at the Chapman-Jouget (CJ) speed, U_{CJ} , as derived in detonation textbooks (e.g., Lee, 2008). Trailing the detonation is the Taylor expansion that terminates on the characteristic moving at sound speed c_3 , the sound speed in the constant pressure region behind the expansion. Since $c_3 < U_{CJ}$, the expansion broadens as the detonation wave. Using the CJ state and the method of characteristics, the spatial and temporal distribution of pressure and fluid velocity may be solved for explicitly (Lee, 2008).

Hence the pressure and fluid velocity are known for all times prior to the detonation reaching the tube end. When the detonation impacts the end wall, a reflected shock wave is created to bring the gas immediately behind the detonation wave to rest. This reflected shock travels in the opposite direction as the detonation. If we are only interested in the shock for times soon after the detonation reflects, then it is possible to make some simplifying assumptions and thereby create a model for the amplitude of the reflected wave as done by Karnesky (2010).

One-dimensional numerical simulations of the reflecting shock (see Section 6) predict that there is a very small pressure gradient between the reflected shock and the end wall until the shock reaches the tail of the expansion. Based on this observation, we made the approximation that there is zero pressure gradient behind the reflected shock so that the pressure just behind the shock is equal to the pressure at the end wall for all times. This approximation is only valid for sufficiently short times following reflection when the shock is still in the Taylor wave. For later times, an expansion wave will develop behind the reflected shock and the pressure gradient cannot be neglected.

Assuming that the pressure P_R behind the reflected shock is known, we can use the shock jump relations (Thompson, 1972) to find the speed, U_R , of the reflected shock. The result is

$$U_R(t) = -u(x,t) + c(x,t) \sqrt{\frac{\gamma+1}{2\gamma} \left[\frac{P_R(t)}{P(x,t)} - 1 \right] + 1} \quad (1)$$

where $u(x,t)$, $P(x,t)$, and $c(x,t)$ are the velocity, pressure, and sound speed just upstream of the shock, as determined by the Taylor wave solution. The shock's trajectory may then be determined by integration.

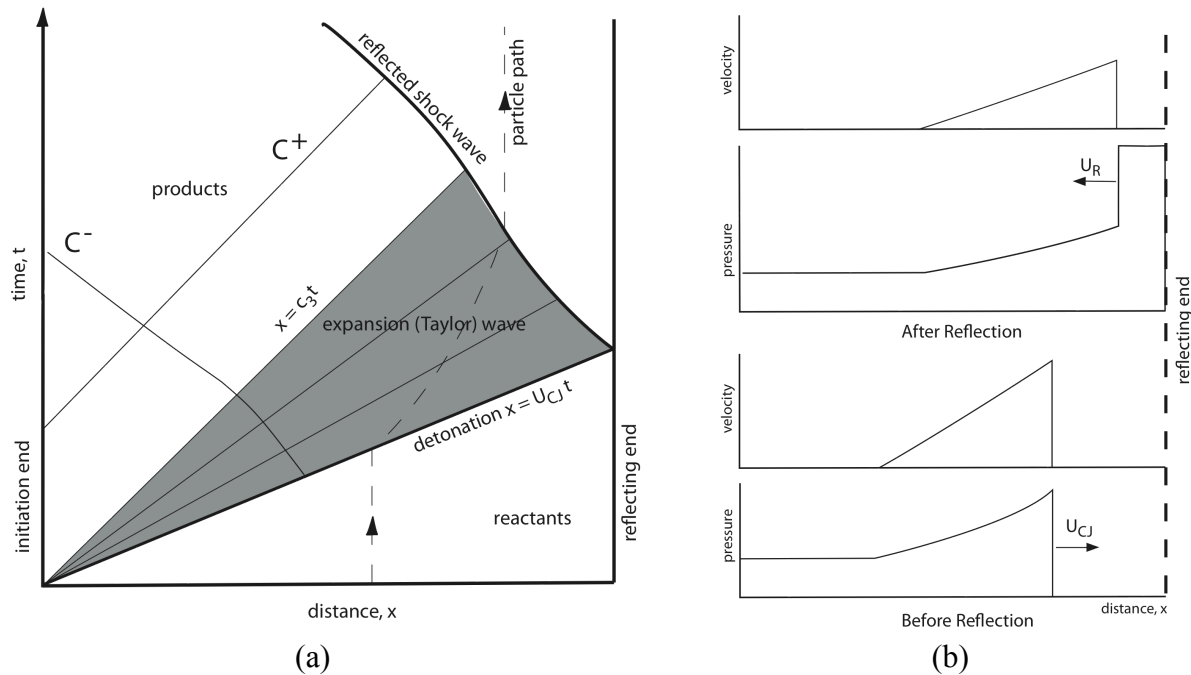


Figure 1. (a) Space-time diagram of an ideal detonation and Taylor wave. (b) Spatial pressure distributions for several times after detonation initiation and prior to reflection.

To use our method of computation, the pressure-time history of the shock must be known from either experimental measurement or simulation. Using the zero-pressure gradient assumption discussed above, the present results approximate the reflected shock pressure as the measured pressure history at the end wall. In practice, the tabulated data of the pressure measurements is inconvenient for numerical simulation, thus we have fit the pressure history to a simple exponential decay of the form

$$P_R(t) = (P_{CJ,ref} - P_3) \exp\left[-\frac{t - t_{ref}}{\tau}\right] + P_3 \quad (2)$$

In order to limit the number of parameters that must be obtained from experimental data, we have based the peak pressure on the computed value $P_{CJ,ref}$ for the ideal reflection of a CJ detonation and also used the computed value of P_3 . These computations were performed using Cantera (Goodwin, 2003) with the Shock and Detonation Toolbox (Browne et al., 2008). The decay constant τ is found by fitting the measured pressure trace to Eqn. (2). Combining this solution for the reflected wave with the previous analytical solution for the Taylor wave, the pressure $P(x,t)$ within the tube is entirely specified.

3. Experimental Setup

The detonation tube used in this series of experiments is an assembly of two tubes of inner diameter 127 mm joined in the center by a gland seal as shown in Figure 2. The left-hand tube has a 25.4 mm wall thickness. This serves as the driver tube wherein ignition takes place via a glow plug in the left-hand wall. The driver tube also contains paddle-shaped obstacles to give

prompt deflagration-to-detonation transition (DDT) thereby ensuring a well-formed detonation enters the right-hand specimen tube, of wall thickness 1.6 mm. At the right-hand side of the specimen tube is a tapered steel ring that squeezes a collet and clamps onto the specimen tube, which in turn presses onto an aluminum plug, with at least a 66 kN clamping force. The plug is mounted to a 2000 kg mass, ensuring a nearly rigid boundary condition at the right hand side. The primary purpose of this test facility was to examine plastic deformation created by reflected detonation waves at higher initial pressures, see Karnesky et al. (2010).

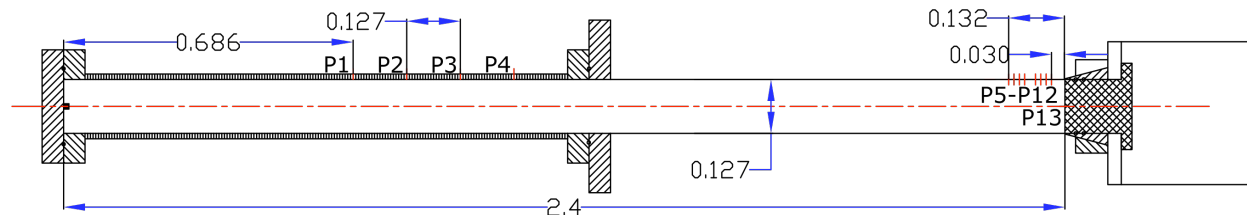


Figure 2. Schematic of detonation tube, dimensions in meters.

For the purposes of examining the dynamics of the reflected waves, the specimen tube is outfitted with thirteen pressure gauges. Four of these are in the driver tube (P1 through P4) and are of type PCB113A24. The remaining nine pressure gauges are located in the specimen tube within the last 150 mm from the location of detonation reflection. Gauges P5 through P12 are of type PCB113A26 and are located in the specimen tube wall and P13, type PCB113A23, is placed in the center of the reflecting end. This enables us to measure the wall pressures generated by the incident and reflecting waves. A complete list of gauge locations is given in Table 1.

Before each experiment, the tube assembly is evacuated before being filled with stoichiometric ethylene-oxygen via the method of partial pressures to an initial total pressure of 50 kPa. Following ignition, we observe a well-formed detonation has already developed when the combustion wave reaches pressure gauge P1, indicating DDT occurs prior to any pressure measurements.

Gauge distance from reflecting end, m	P1	P2	P3	P4	P5	P6	P7
	1.686	1.559	1.432	1.305	0.133	0.121	0.108
	P8	P9	P10	P11	P12	P13	
0.095	0.070	0.057	0.044	0.032	0.000		

Table 1. Pressure gauge locations.

4. Experimental Results

Figure 3 illustrates the typical pressure profiles observed in an experiment. The blue and red lines are pressure recordings from two different experiments, these are overlaid to illustrate the repeatability in the pressure data. The initial rise in pressure for gauges P5 through P12 marks the arrival time of the detonation. From these measurements, we can extract the detonation wave speed to be $U_{det} = 2348$ m/s. The theoretical CJ velocity as determined by the Shock and Detonation Toolbox (Browne et al., 2008) is 2339 m/s; which is only a 0.4% difference from the measured speed. The time when the detonation reaches the reflecting end is determined by the

initial rise in pressure on gauge P13. Gauges P5 through P12 then track the reflecting shock wave as it travels away from the reflecting end. In Figure 3(a), the fit of P_R to P13 was based on the theoretical values of peak and plateau pressures, which resulted in an accurate prediction of the arrival time of the reflected shock wave to within the rise time of the pressure trace.

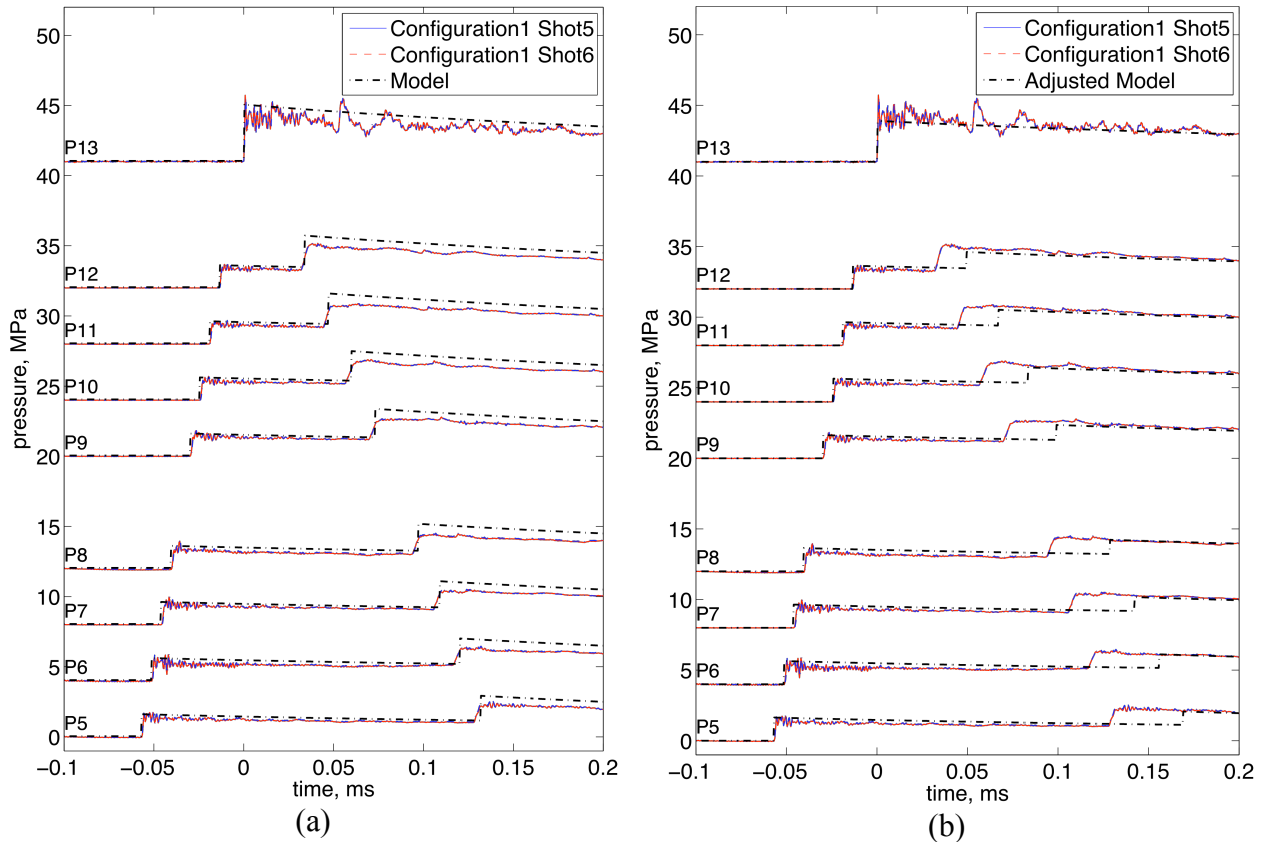


Figure 3. Pressure data compared to model results using two different end-wall pressure histories. Vertical offsets are proportional to the physical separation of the gauges.

Although we are accurately predicting the shock speed, we observe that the measured wall pressure is approximately 20% below that predicted by one-dimensional theory. In other words, the speed of the reflected shock wave is inconsistent with the pressure data measured at the wall of the tube. If we vary the parameters of peak and plateau pressure to more accurately fit the recorded shock amplitudes, we get the profiles shown in Figure 3(b). Now the pressures are accurately predicted, but the shock speed is not. It is also noteworthy that the measured rise time of the pressure of the reflected shock is slower than expected—four times longer than the rise time of the incident detonation wave.

These discrepancies suggest that the pressure is not uniform across the tube and the shock waves are not one-dimensional. One possible reason for these discrepancies is the viscous boundary layer that will be present at the tube wall. The reflected shock wave may be interacting with the boundary layer to create a multi-dimensional wave front near the reflected end. Such effects have been observed in shock tubes where interaction of the reflected shock wave with the boundary

layer set up by the incident shock results in separated flow with an oblique shock in the boundary layer leading the main reflected wave (Mark, 1958; Petersen and Hanson, 2006).

5. Reflected Shock Wave—Boundary Layer Interaction

A sketch of reflected shock wave—boundary layer interaction is shown in Figure 4. The incident detonation induces a velocity in the fluid, Figure 1(b). The no-slip condition requires the velocity be zero at the wall and thus a boundary layer is created. The reflected shock wave propagates into the flow outside the boundary layer in an essentially one-dimensional fashion. Near the wall, the combination of low-speed fluid in the boundary layer and the pressure rise across the reflected shock wave can result in the separation of the flow. A system of oblique shocks is created to equilibrate the pressures in the region next to the end wall. The leading portion of the reflected shock wave that passes through the boundary layer (shock wave O in Figure 4) is an oblique wave and a reflected wave (R) is observed where this joins the normal (N) shock wave. This configuration resembles the shock bifurcation or lambda shock observed in the more familiar process of shock wave—boundary layer interaction in supersonic steady flow.

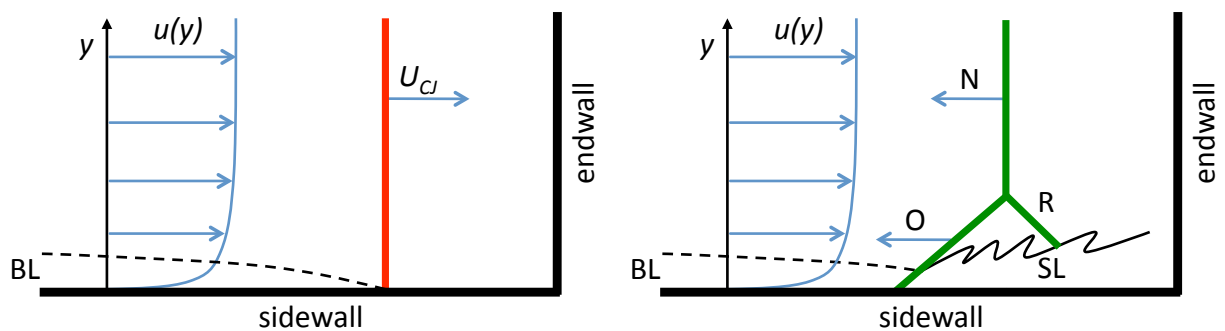


Figure 4. Schematic of flow for bifurcated shock wave.

Experiments in non-reacting flow show that boundary layer separation and oblique shocks only occur under certain conditions. Mark (1958) developed a simple criterion for when shock waves bifurcate. He theorized that bifurcation will occur if the stagnation pressure in the boundary layer in the shock-fixed frame is less than the pressure behind the normal shock. When using this criterion, it is necessary to determine the Mach number of the reflecting shock wave in the boundary layer. When we attempt to apply this to reflecting detonations, we encounter a serious difficulty because of the temperature dependence of the sound speed and the Mach number with distance from the wall. Mark considered relatively weak shock waves and assumed that the sound speed within the boundary layer remains constant. However this assumption is not valid in the case of reflecting detonations due to the large temperature variations within the boundary layer. To resolve this issue and investigate the conditions under which boundary layer separation occurs for detonation reflection, it is necessary to consider the unsteady interaction of the reflected shock wave with a compressible viscous flow, described in the next section.

6. Computational Results

Two types of simulations were performed. A non-reactive, one-dimensional Euler (inviscid) simulation was carried out in order to have a reference solution for comparison to experiments and the full two-dimensional, viscous simulations. The main simulations were two-dimensional viscous compressible reactive computations of an incident detonation wave reflecting from a planar end wall and also setting up a boundary layer on the sidewall. Both simulations used simplified models of the chemical reaction process and considered idealized detonation waves with reaction zones, but using parameters that did not result in unstable detonation fronts. Although highly idealized, we believe that these models do provide insight into the key physical processes.

Our simulations utilized the fluid-solver framework, AMROC (Adaptive Mesh Refinement in Object-oriented C++), version 2.0, integrated into the Virtual Test Facility (Deiterding et al., 2005), which is based on the block-structured adaptive mesh refinement algorithm of Berger and Olinger. This algorithm is designed especially as a framework for the solution of hyperbolic partial differential equations with parallelized structured adaptive-mesh refinement (SAMR). The numerical method used with this framework is a hybrid 6th-order accurate Centered-Difference(CD)/WENO finite difference method (Ziegler, 2010). A shock detection algorithm enables WENO use only at strong shocks allowing the inexpensive CD method to be used in all smooth flow regions. Integration is carried out with 3rd order time accurate SSP RK3 along with time-splitting for the reactive source terms.

A simple thermo-chemical mechanism was designed to model a H₂, O₂, Ar detonation with pressure ratios of 2, 1, and 7 at a state with a pressure and temperature of 50 kPa and 298 K. Using a high temperature extension of the GRI30 mechanism in Cantera (Goodwin, 2003) and the Shock and Detonation Toolbox (Browne et al., 2008), a ZND solution was calculated with detailed chemistry. A fitting procedure was used together with this solution to determine approximate parameters for a one-step Arrhenius model with simple depletion rate for the modeled chemical reaction. For this two-species model, the total energy is defined by the heat release per unit mass parameter, q . Viscosity, conductivity, and mass diffusion were calculated by the Sutherland model (White, 1974).

The approximate two-species mechanism properties were fitted to match the detailed mechanism's ZND solution properties at one-half the reaction length. The gas and chemistry parameters used are given below in Table 2. These values correspond to a post shock von Neumann pressure of approximately 1.42 MPa and detonation shock speed of $U_{shock} = 1774$ m/s. The reference values for viscosity, thermal conductivity, and mass diffusion were selected by matching values at the end of the reaction zone. This yields the following reference properties: $T_{ref} = 2700$ K, $\mu_{ref} = 1.07 \cdot 10^{-4}$ Pa·s, $k_{ref} = 0.148$ W/(m·K), $D_{ref} = 6 \cdot 10^{-4}$ m²/s.

T_{∞} , K	P_{∞} , kPa	γ	W , kg/mol	q , J/mol	E_a , J/mol	A , s ⁻¹
298	50	1.4333	0.031	43000	30000	125000

Table 2. Gas and chemistry parameters used in computations.

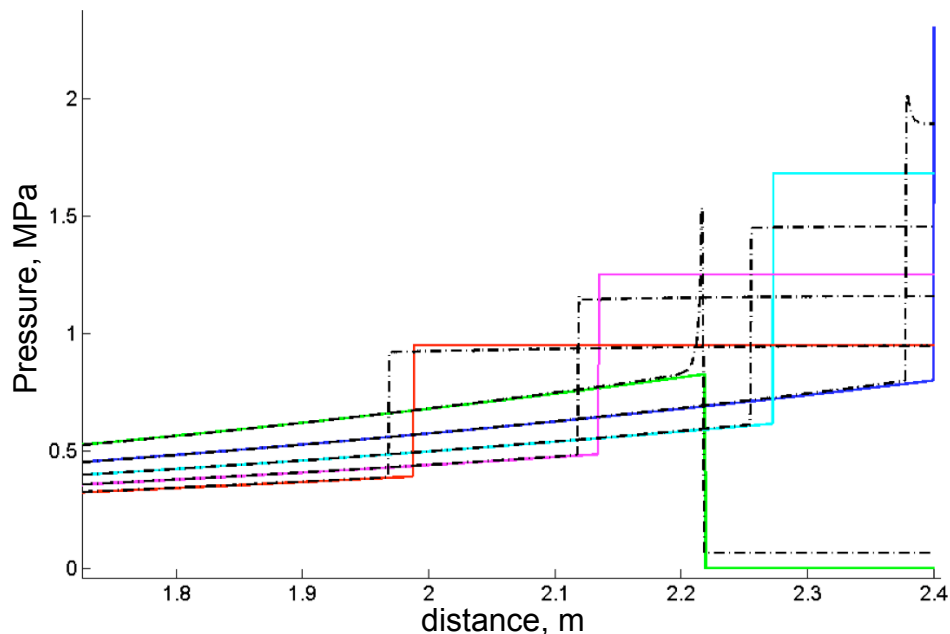


Figure 5. Comparison of the approximate pressure model, $P_R(x)$ to the 1D reactive Euler simulation of the TZ wave for a tube of length 2.4 meters with $\tau = 3000$, and a reflected shock pressure of 2.45 MPa, the approximate reflected value for the CJ post detonation state (the reflected von Neumann state is 8.86 MPa).

Shown in Figure 5 is the comparison between the 1D reactive Euler simulations and the approximate analytic pressure model. As assumed in the simple model, the gradient in pressure between the shock and the end wall is extremely small and the model approximations are reasonable. Overall, the agreement of the model and the one-dimensional inviscid calculations are reasonable. As found with the experimental results, both the reflected shock speed and the reflected shock amplitude could not be exactly matched. The source of this discrepancy is still being examined.

The 2D simulations were carried out using the ZND initial condition starting in a domain of 40x40 mm. Four mesh refinement levels were used, for which case the smallest cell size was $7.8 \cdot 10^{-3}$ mm. These results were not fully resolved, however, enough cells were used across the boundary layer to gain insight into the overall flow properties.

Figure 6 clearly shows that the boundary layer separates and a bifurcated reflected shock wave develops. The basic structures discussed earlier in connection with non-reactive shock waves are clearly visible. These include the oblique shock propagating ahead of the main wave that is slightly curved and a reflected oblique wave extending from the triple point nearly to the wall. A series of vortices are visible near the wall and appear to be the result of the rolling up of the vortical boundary layer fluid. A number of weak shock waves can be observed propagating away from the interaction region towards the center of the flow.

As shown in Figure 7 the pressure at the wall is significantly different than either the pressure in the center of the flow or the reference inviscid solution. The pressure at the wall clearly shows

the lower amplitude oblique shock wave propagating ahead of the normal shock in the core flow. A series of pressure oscillations are visible which appear to be associated with the vortices moving along the wall and are terminated by a sharp rise associated with the reflected shock wave. The amplitude and timing of the one-dimensional inviscid solution is in good agreement with the wave form in the core of the two-dimensional viscous flow. This indicates that at this particular time, the viscous effects are still confined to the walls. The pressure traces shown in Figure 7 confirm our speculations regarding the potential effects of reflected shock—boundary layer interaction on side wall pressure histories.

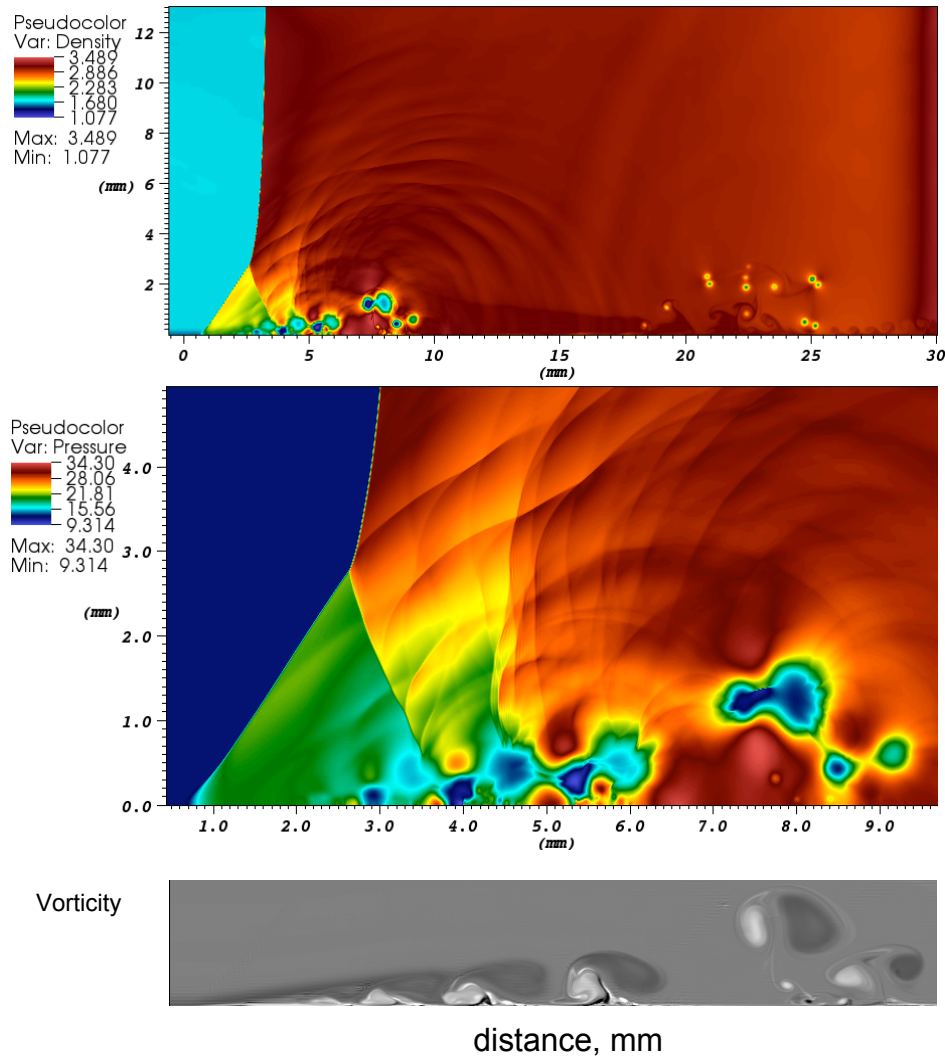


Figure 6. 2D reflected detonation: Density, pressure, and vorticity pseudo color plots (non-dimensional units) of the shock bifurcation from a detonation reflection at 50 kPa initial pressure. The reflecting end wall is at $x=30$ mm.

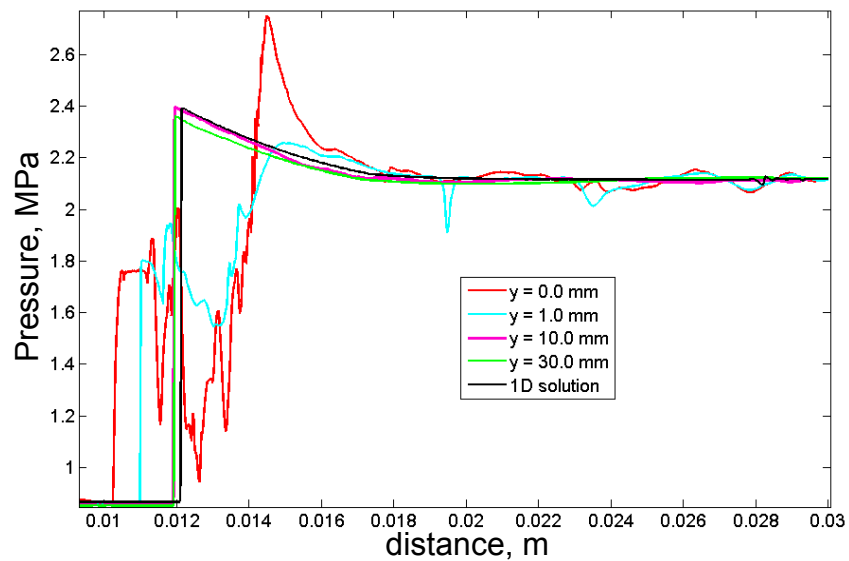


Figure 7. Pressure traces at the heights of 0, 1, 10, and 30 mm from the wall $2.56 \cdot 10^{-5}$ s after reflection.

7. Conclusions

Pressure measurements during detonation reflection are inconsistent with one-dimensional inviscid gas dynamic models. There is an inconsistency between the measured shock speed and the measured shock pressures if the flow is one-dimensional. We conclude that the pressure jump across the shock wave is larger in the center of the tube and there is a weaker shock wave leading the main front at the tube walls.

A two-dimensional viscous compressible simulation of the reflection process clearly demonstrates reflected shock wave—boundary layer interaction can result in separated flow and bifurcation of the reflected wave front. We observe many of the same features in the computational pressure traces as in the measured pressure histories. These include the increase in the rise time of the pressure and the inconsistency between measured wave speed and pressures inferred from one-dimensional inviscid models.

The present results report on a work in progress. Planned future activities include incorporating these findings into improved models of pressure wave loadings of structural response simulations. We also plan to carry out visualization experiments to gain further insight into the reflection process and for validation of the numerical simulations.

Acknowledgements

This research is sponsored by the Department of Homeland Security through the University of Rhode Island, Center of Excellence for Explosives Detection. J. Damazo is supported by an NDSEG Fellowship and J. Zeigler is supported by a DOE CSGF Fellowship.

References

- Beltman WM, Shepherd JE. Linear elastic response of tubes to internal detonation loading. *J Sound Vib* 2002;252:617–55.
- Chao TW, Shepherd JE. Comparison of fracture response of preflawed tubes under internal static and detonation loading. *J Press Vessel Technol* 2004;126(3):345–53.
- Deiterding R, Bader G. High-resolution simulation of detonations with detailed chemistry. In: Warnecke G, editor. *Analysis and numerics for conservation laws*. Magdeburg: Springer; 2005. p. 69–91.
- Fickett W, Davis WC. *Detonation: Theory and experiment*. Toronto: Dover; 2001.
- Goodwin DG. Cantera – An open-source, extensible software suite for CVD process simulations. *Electrochem Soc* 2003;155–162.
- Karnesky J. *Detonation induced strain in tubes [dissertation]*. Pasadena, CA, USA: Calif Inst of Technol; 2010.
- Karnesky J, Damazo J, Shepherd JE, Rusinek A. Plastic response of thin-walled tubes to detonation. *Proceedings of the ASME 2010 Pressure Vessels and Piping Conference*; 2010 Jul 18-22; Bellevue, USA.
- Lee JHS. *The detonation phenomenon*. New York: Cambridge University Press; 2008.
- Mark H. The interaction of a reflected shock wave with the boundary layer in a shock tube. Ithica, NY, USA: Cornell University; 1958 Mar. NACA TM1418. 1958.
- Petersen EL, Hanson RK. Measurement of reflected-shock bifurcation over a wide range of gas composition and pressure. *Shock Waves* 2006;15:333–40.
- Shepherd JE, Teodorczyk A, Knystautas R, Lee JHS. Shock waves produced by reflected detonations. *Prog in Astronaut Aeronaut* 1991;134:244–64.
- Thompson PA. *Compressible fluid dynamics*. New York: McGraw-Hill; 1972.
- Wintenberger E, Austin JM, Cooper M, Jackson S, Shepherd JE. Reply to ‘Comment on analytical model for the impulse of single-cycle pulse detonation tube’. *J Propuls Power* 2004;20(5):957–9.
- White FM. *Viscous fluid flow*. New York: McGraw-Hill; 1974.
- Ziegler J, Deiterding R, Pullin D, Shepherd JE. High-order hybrid scheme for compressive, viscous flows with detailed chemistry. Submitted to *J Comp Physics*; 2010.